OATAO is an open access repository that collects the work of Toulouse researchers and makes it freely available over the web where possible

This is an author's version published in: http://oatao.univ-toulouse.fr/20233

Official URL : https://doi.org/10.1016/B978-1-78242-028-6.00025-9

Any correspondence concerning this service should be sent to the repository administrator: tech-oatao@listes-diff.inp-toulouse.fr

Ultrasonic mixing, homogenization, and emulsification in food processing and other applications

H. Delmas, L. Barthe
Laboratoire de Génie Chimique, Toulouse, France

25.1 Introduction

The use of power ultrasound (US) to intensify physicochemical processes is now a large area of research. The most famous application of high-power US is cleaning, but many other processes may be dramatically enhanced or qualitatively improved by ultrasonic irradiation. Various industrial fields are concerned as materials ([nano]materials, polymers, surface coatings, and electrochemistry), the environment (especially water, sludge, and soil treatments), and cosmetic and food engineering (mainly through extraction of natural products from plants, dissolution, homogenization, and emulsification processes). Among these various applications of power US the main unit operations most often involve multiphase media for either production and/or dispersion of a solid phase in a liquid through precipitation, crystallization, or simple deaggregation or disruption and/or dissolution of particles, floc, curd, and cells. These operations may be highly improved by power US.

This chapter analyzes the effects of power US on such physical operations, excluding any reactive process. First, it has to be emphasized that hydrodynamics connected with power US does control its mechanical effects through acoustic cavitation, a key phenomenon, and through acoustic streaming, albeit to a much lesser extent. Thus a brief survey of cavitation and acoustic streaming gives the minimum information necessary to understand local and global US-induced hydrodynamics. As a direct consequence of acoustic cavitation and streaming, US mixing—both at a reactor scale (macromixing) and a molecular scale (micromixing)—is presented, with reference to the engineering approach linking cavitation and acoustic streaming phenomena to micro- and macromixing, respectively.

Concerning specific US applications for solid–liquid suspensions, dispersion, or deagglomeration, the process of separating and suspending tiny particles that are initially naturally aggregated by attraction forces, is reviewed first. Then particle size reduction, achieved either by mechanical erosion/disruption or by dissolution, is detailed, including the combination of simultaneous disruption and dissolution. Rather similar applications concerning cells disruption and the dissolution of their organic content, especially for sludge treatment, are detailed. Finally, two main

.

applications of the general principles of homogenization and emulsification are developed. Homogenization is an important unit operation in food engineering to reduce the size of particles and globules in milk, fruit juice, tomato products, and sauces. Here only US milk homogenization, the main case by far, is detailed. US emulsification is then specifically emphasized. It consists of intimately mixing two liquid phases (at least) to achieve a stable concentrated suspension of droplets. This operation has important applications in the food and cosmetic industry by creating new complex media with specific end use properties.

25.2 Cavitation and acoustic streaming

25.2.1 Acoustic cavitation

It is now clearly stated that most of US outstanding effects are due to transient acoustic cavitation. Transient acoustic cavitation is a very complex highly nonlinear phenomenon which occurs at given acoustic pressure conditions (needing rather high US intensity—about 1 W/cm^2 in water at room conditions). Microbubbles are generated from nuclei—favored by dissolved gas, wall defects, and liquid impurities—during the low-pressure half periods (bubble expansion). They may oscillate for a few periods, undergoing slow average growth through the so-called rectified diffusion process (up to several micrometers) and, having reached a critical size, they suddenly dramatically grow during the low-pressure half period and collapse violently in a very short fraction of the high-pressure half period. Most often the bubble breaks up after collapse, reproducing the same scenario for smaller bubbles: oscillatory growth driven by rectified diffusion then sudden collapse. Because such fast collapse is nearly adiabatic, it gives rise to extreme conditions inside and around the collapsing bubble: up to 5000 K at the bubble center, 1000 bar, a high radial velocity up to sound speed and then shock waves as the bubble rebounds (according to single-phase models or high-velocity video recording). These cavitation characteristics have different impacts on the sonicated media: high temperature peaks produce very active free radicals (mainly OH$^.$ in aqueous media), giving way to intense radical chemistry either inside or at the interface of the cavitation bubble, depending on the volatility of the dissolved target molecules. High-pressure, high-velocity gradients and shock waves have mainly physical effects through very strong microturbulence and intense local mixing, increasing heat and mass transfer. These physical effects are even more efficient in multiphase systems and especially on solid surfaces because of asymmetrical collapse, with the projection of a fast jet toward the solid close to the cavitation bubbles. This is the main mode of action in ultrasonic cleaning and most ultrasonic solid processing.

The main parameters affecting cavitation are either related to US emission (US power or, more likely, power intensity—in W/cm^2—or acoustic pressure and US frequency, generally from 20 to 1000 kHz), to pressure and temperature, and to physicochemical properties of the irradiated medium, such as compressibility, vapor pressure, surface tension, viscosity, nature of gas above the liquid, and multiphase characteristics (fraction of gas, immiscible liquid, dispersed solid).

It has been known for 20 years—and has recently been more precisely quantified—that the two main effects of acoustic cavitation are inversely dependent on US frequency: high frequency is better for chemical activation because free radicals are faster in contact with the reacting molecules because of much smaller cavitation bubbles; low frequency, however, gives rise to much larger bubbles, which collapse more violently and involve greater physical effects.

Although cavitation was clearly proven to be the main cause of US intensification in most multiphase processes, its complete characterization by relevant measurements or through complex calculation (not restricted to single-bubble dynamics) have not received much attention. The main direct measurement of cavitation intensity is performed by a hydrophone, which records and analyzes noise spectra (Brotchie et al., 2010; Guo et al., 2007; Komarov et al., 2013; Moholkar et al., 2000; Son et al., 2012). Such measurements are not simple to read; the hydrophone interacts with the acoustic field and gives an integrated response because of its large size compared to cavitation bubbles. Moholkar et al. (2000) proposed an interesting work on cavitation mapping in an ultrasonic bath and derived the "true" cavitation intensity by subtracting the cavitation noise from the acoustic signal obtained in a noncavitation condition using silicon oil instead of water. The results at many locations in the bath near the free surface were given in terms of acoustic pressure, showing large local variations due to both nonhomogeneous emission at the bottom (low intensity in corners) and significant damping caused by cavitation bubbles.

More information on cavitation properties is given by the characteristics of acoustic cavitation bubbles. Ashokkumar (2011) recently reviewed this topic. Concerning bubble size and velocity in nonstanding wave cavitation, results are still rather scarce since the first works by Burdin et al. (1999) and Tsochatzidis et al. (2001) using laser light diffraction and a phase Doppler granulovelocimeter. The two techniques gave roughly consistent information: along the axis of a 13-mm ultrasonic horn, the mean bubble velocity clearly decreased from 1.5 m/s to a few centimeters per second at maximum US intensity (180 W), and the mean bubble diameter slightly decreasing with US power (from 40 μm at 40 W to about 10 μm at 180 W). The bubble void fraction seems rather difficult to quantify. Near the horn at maximum bubble concentration, the void fraction was as low as 5×10^{-4} with light diffraction and 5×10^{-3} with phase Doppler, whereas recent magnetic resonance imaging measurements (Mastikhin et al., 2012) proposed 8×10^{-3} in same conditions.

25.2.2 Acoustic streaming

The emission of ultrasonic waves gives rise to a forward motion of the fluid. The liquid jet formed on the axis of the emitter (when cylindrical) includes the more concentrated population of acoustic cavitation bubbles because this region is the most irradiated. Velocity was measured with laser Doppler anemometry and particle image velocimetry and showed coherent results: the velocity depends mainly on US density and on liquid or slurry viscosity. In water velocity between 0.1 and 0.3 m/s (Hihn et al., 2011) when the jet impacts a solid surface and up to 1.5 m/s (Kumar et al., 2007) at 70 W on a 13-mm horn, and even up to 2 m/s (Tsochatzidis et al., 2001) near

the emitter surface of a large volume at a much higher intensity (180 W on a 13-mm horn) has generally been reported. Some saturation due to bubble accumulation at the surface often has been mentioned (Hihn et al., 2011), leading to a smaller increase in velocity when increasing too much the power. Concerning the whole velocity field, because of acoustic streaming, like a usual jet, the velocity exhibits a sharp radial profile near the emitting surface and a strong decrease along the axis (Kumar et al., 2007). This acoustic streaming may lead to significant flow and is sometimes strong enough to ensure good mixing and homogeneity in small US apparatus without an additional mixing device (stirrer, pump, static mixer).

25.2.3 Conclusion

Power US in a liquid or a multiphase mixture with a continuous liquid phase may generate two distinct hydrodynamic phenomena: acoustic cavitation and acoustic streaming. Only acoustic cavitation at high acoustic pressure may have a significant effect on the sonicated medium because of the violent collapse of microbubbles, giving rise to hot spots in the gas phase and intense turbulence and shear stresses at the micron scale in the liquid phase. The attraction of the collapsing bubble toward solid surfaces and the possible excess of nuclei near the interface make acoustic cavitation extremely performing in multiphase processes, whereas acoustic streaming may sometimes be used to optimize the overall flow in the sonicated volume; most often, however, it may be ignored in large-scale US processes.

25.3 Mixing

When trying to explain the outstanding performances of some US assisted processes, improved mixing is often cited. Nevertheless, this claim is generally connected with visual observations (Guo et al., 2007; Parvizian et al., 2011; Yusaf and Buttsworth, 2007), although rather few works have actually been devoted to the quantification of mixing under US using conventional engineering criteria. Indeed, mixing should characterize the degree of homogeneity of either a single phase or a multiphase medium and may be quantified either at the overall apparatus scale (as a mixing time in a batch condition or a dispersion of the residence time distribution [RTD] in continuous operation)—referred to as macromixing—or at much lower scale (e.g., particles or droplets) and referred as micromixing. The quality of micromixing has a major effect on many phenomena occurring at the submicronic scale: precipitation, emulsification, mass transfer at interfaces, reaction rate, and selectivity.

25.3.1 Macromixing

Depending on whether the process is batch or continuous, macromixing is characterized by a mixing time (time to obtain a quasi-homogeneous concentration from mixing) or by the variance of the RTD. The dimensionless variance of RTD, σ^2, ranging from 0 for perfectly unmixed flow (plug flow) to 1 in perfectly mixed flow, often is

used to obtain either the number N of equivalent perfectly stirred tanks in a series ($N = 1/\sigma^2$) or the Péclet number, based on the axial dispersion model.

$$Pe = \frac{L\,v}{D_A} \approx \frac{2}{\sigma^2} \tag{25.1}$$

where L is defined as the reactor length (m), v is the average fluid velocity (m/s), and D_A is the axial dispersion (m²/s). Both criteria (mixing time or σ^2) are obtained through tracer experiments. In batch operation the mixing time is the time needed to reach a quasi-uniform concentration (e.g., 90% or 95% of the average final concentration) after tracer injection. Of course, this mixing time may depend on the location of both the tracer injection and the tracer detection. Mixing time is the most important criterion concerning homogeneity at the apparatus scale, but it does not reflect the quality of mixing at the molecular scale (micromixing), which may govern the reaction rate and selectivity, as mentioned earlier. To simplify, it may be assumed that macromixing results from the velocity field in the reactor, which is mainly governed by stirring or pumping and, in small-scale US equipment, by acoustic streaming, especially with a small horn and high US intensity. Few works have been devoted to macromixing under US (Murugan and Nagarajan, 2008; Vichare et al., 2001; Yusaf and Buttsworth, 2007), probably because of a rather poor US effect. Indeed, Vichare et al. (2001) concluded that, without any stirring or pumping, the mixing time evolution versus a Reynolds number based on horn tip diameter and average liquid circulation velocity is very similar to the one observed in a simple jet. A complete correlation was proposed based on mixing in a simple jet flow involving the diameter and height of the tank, the diameter and location of the horn on the tank axis, the viscosity and density of the fluid, and the horn's vibration velocity. The same type of result with a minor effect of US on RTD was found in a tubular flow reactor at a high US frequency (Parvizian et al., 2012).

US does not significantly improve macromixing because the acoustic streaming velocity is generally one order of magnitude lower than the velocity achieved by mechanical devices (stirrer or pump) in large US reactors. Conversely, it is important to get a good mixing in any US apparatus when acoustic energy is not homogenously distributed, which is most often the case (Kojima et al., 2010). Good mixing forces the fluid or mixture being treated to pass regularly through the best irradiated zones and therefore improves the overall effectiveness of US. Alternatively, premixing with conventional equipment could be dramatically helpful, as in emulsification (see Section 25.7).

25.3.2 Micromixing

Micromixing is linked to small-scale turbulence and velocity gradients, and, compared with macromixing, it is dramatically affected by intense cavitation when using power US (Yusaf and Buttsworth, 2007). Contrary to macroscopic hydrodynamics, micromixing cannot be measured directly because of microsensor limitations. Experiments are based on chemical selectivity when carrying out either consecutive competing reactions (A+B→R and R+B→S) or parallel competing reactions (A+B→R and

C+B → S). In the two schemes the first reaction is extremely fast, whereas the second is moderately fast. With an excess of A, and in perfectly mixed conditions, all B should be consumed by the first reaction and no S should be formed. From C_s (the experimental final concentration of S), a micromixing or segregation index $X_s \sim C_s$ may be calculated and linked to turbulence theory with the convenient model of engulfment-deformation-diffusion (Baldyga and Bourne, 1984). This model links X_s and the micromixing time t_m. The first works on US micromixing (Monnier et al., 1999a,b) and later ones (Parvizian et al., 2011, 2012) were conducted with a competing scheme: the so-called Dushman reaction. Other works used precipitation reactions (Pohl et al., 2012a,b).

Micromixing in jets or stirred tanks results from the transmission of kinetic energy from the large eddies to the smaller ones, down to the Kolmogorov scale, defined as $\eta = (\nu^3/\varepsilon)^{1/4}$, where ε is the dissipated power per unit mass (in W/kg) and ν is the kinematic viscosity. Viscosity dominates at the Kolmogorov scale, and the turbulent kinetic energy is dissipated into heat. Under this scale molecular diffusion completes the homogenization. The transmission of energy in acoustic cavitation occurs differently: acoustic bubble collapses directly concentrate very high amounts of energy at the micron scale. Nevertheless, the engulfment-deformation-diffusion model conveniently represents the evolution of micromixing time in both situations (Monnier et al., 1999a).

It was clearly demonstrated that power US strongly enhances micromixing by dramatically reducing the segregation index, especially at low frequencies (20 kHz), whereas frequencies of 514 and 1000 kHz were much less efficient. Figure 25.1 shows the effect of energy dissipation on mixing time for three reactor volumes. Interestingly, at the same energy dissipation (then the same energy density), better micromixing was achieved in larger volumes. When compared to classical stirring with a Rushton turbine, US was not competitive at the highest volume tested because it needed about two to three times more energy to reach the same micromixing quality (Figure 25.2). By extrapolating Figure 25.1 toward higher volumes, it might be
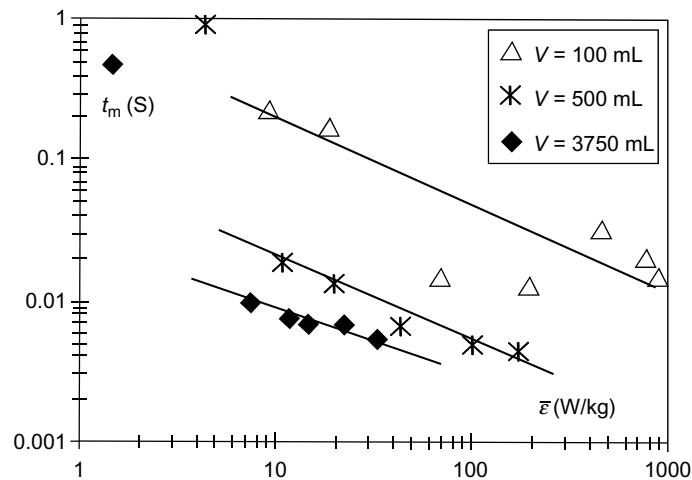

Figure 25.1 Characteristic micromixing time t_m versus global energy dissipation rate for three volumes, (probe-horn, $f = 20$ kHz, $T = 273$ K), according to Monnier et al. (1999b).
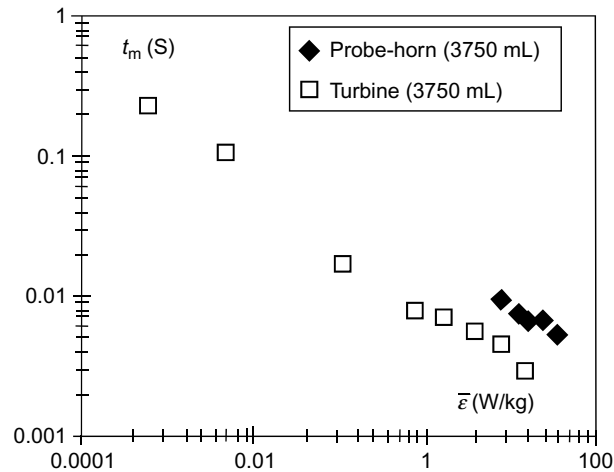
Figure 25.2 Micromixing time t_m versus global rate of dissipated energy both probe-horn (20 kHz) and mechanical stirring (Rushton turbine), according to Monnier et al. (1999b).

supposed that US could become more attractive than usual stirring because of its focused energy dissipation near the injection (and reaction zone); stirring spreads more turbulent energy throughout the whole reactor volume. Another interesting use of US to improve fast reaction selectivity is to develop a small continuous reactor (Figure 25.3) in which high US energy may be confined and added to natural mixing

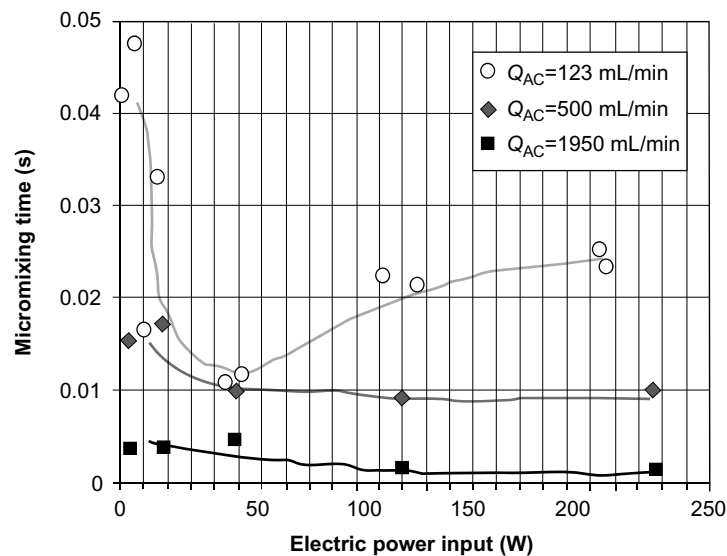**Figure 25.3** Influence of the input electric power versus the micromixing time for three flow rates $Q_{AC} = 123$, 500, and 1950 mL/min ($a = 10$ mm, $d = 13$ mm, $f = 20$ kHz), according to Monnier et al. (2000).

through the two reactor feds. The quality of micromixing in conventional flow reactors depending mainly on flow rates and the size of injectors was clearly improved by US, especially at low flow rates and even at low input power. As often observed in many applications, too much power may have a negative effect. It also was shown that in such US reactors the negative effects of viscosity on micromixing could be significantly reduced (Monnier et al., 2000).

25.4 Particle and aggregate dispersion and disruption

US has been extensively used for chemical effects, but physical and mechanical effects, including particle and aggregate dispersion and disruption, have more recently been investigated. These two phenomena are controlled by the same main mechanisms involving shocks and particle separation or breakup: on the one hand, vibration and implosion of the cavitation bubbles and, on the other hand, collisions between suspended particles.

25.4.1 Dispersion or deagglomeration

Nanomaterials such as nanoparticles are increasingly used because of interesting properties such as a large specific area. Therefore it is imperative to produce and keep them individually avoiding agglomeration; US may be convenient for both. Before discussing US effect for dispersion or deagglomeration, it is interesting to point out that sonication can play an important role in the preparation step. US physical effects can improve considerably this stage. Indeed, acoustic cavitation permits chemical reactions under extreme conditions of temperature and pressure, as reported in Section 25.2. In addition, mass transfer is enhanced by acoustic streaming. Numerous reviews deal with the sonochemical preparation of nanomaterials (Bang and Suslick, 2010; Gedanken, 2004; Suslick and Price, 1999; Suslick et al., 1996; Xu et al., 2013). Sonication is chosen for the preparation of nanostructured metals, alloys, oxides, carbides and sulfides, colloids, and catalysts, among others, and this area is expanding quickly. In particular, sonication is well known to be advantageous in sonocrystallization because US reduces the induction time of nucleation, ensuring the formation of many small crystals and preventing their agglomeration. Moreover, the cooling rate in the liquid at the bubble surface is very high (10^8 K/s), and collapse occurs in about a nanosecond. This could play a significant part in increasing supersaturation (De Castro and Riego-Capote, 2007; Ruecroft et al., 2005).

The dispersion or deagglomeration of (nano)particles into liquids such as aqueous solutions is required for a variety of applications: catalysis, pharmaceutics, cosmetics, and paints, to name a few. However, the attracting electrostatic forces (e.g., van der Waals forces) get stronger as the particles size decreases, so nanoparticles tend to form agglomerates. Mechanical stirrers are conventionally used for the dispersion of particles into liquids. This includes high-pressure homogenizers, stirred bead mills, and rotor-stator mixers. Nevertheless, they are not sufficient in the case of nanoparticles. Sonication at a low frequency is an interesting alternative to these techniques

(Guo et al., 2007). In this case, as explained previously in Section 25.2, acoustic cavitation creates micron-sized cavitation bubbles, which collapse violently. These shear forces break particle agglomerates into single dispersed particles. Even if US succeeds in disrupting the agglomerates, the use of stabilizers seems necessary to avoid re-agglomeration. Indeed, to maintain a stable suspension, salts are used for electrostatic stabilization and surfactants or dispersants for steric stabilization to maintain good dispersion (Fasaki et al., 2012). However, it is assumed that inter-particle bonding is not the same for initial agglomerates and for agglomerates formed during sonication. In the second case, the dispersant is sufficient to break them.

One parameter that is particularly important during cavitation and of special influence for deagglomeration and dispersion is the gas content in the liquid. This dissolved or dispersed gas facilitates cavitation through the availability of gas nuclei. These nuclei provide the basis for bubble formation and growth and so decrease the cavitation threshold. Moreover, the nanoparticle agglomerates contain crevices and recesses that can trap the vapor–gas nuclei (see Figure 25.4). The acoustic cavitation can start inside or around the agglomerates (Mason and Lorimer, 2002). This results in more efficient deagglomeration.

Another key phenomenon is shock waves accelerating solid particles suspended in the liquid. Interparticle collisions are very violent and can reach a high velocity (200 m/s). This results in the separation of the agglomerates and modification of particle morphology and surface composition. It is important to note that in particular cases, this phenomenon can cause the opposite effect. Indeed, metal microparticles hitting each other at such a high speed can induce local melting at the collision point and generate agglomeration. However, it can only happen in the case of metals with a low melting point ($<700°$K) such as zinc and tin and a specific particle size (a few microns). These collisions under US were carefully investigated (Doktycz and Suslick, 1990; Prozorov et al., 2004). It is noteworthy that the collapses are more violent at a high external pressure, which can be an interesting operation parameter (Sauter et al., 2008).

US can be used to deagglomerate and disperse different kinds of particles in suspension, for example, metallic oxide (Pohl et al., 2004), ceramic (Chartier et al., 1991), soil (Hereter et al., 2002; Roscoe et al., 2000), and carbon nanotubes (Cheng et al., 2010; Krause et al., 2010). For the latter, it is important to note that
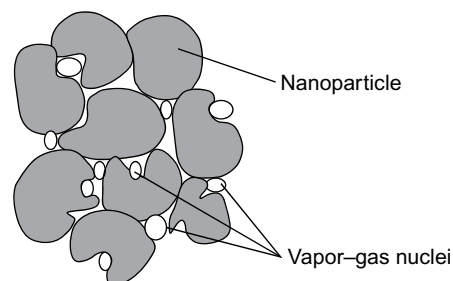

Figure 25.4 Vapor–gas nuclei trapped in crevices and recesses of nanoparticle agglomerates, according to Mason and Lorimer (2002).

Table 25.1 **Specific energy and final mean diameter obtained under ultrasonic conditions for different kind of particles**

Particle nature	Power (W)	Time (min)	E_v (J/L)	Final mean diameter (μm)
Aluminum oxide	360	2	4.3×10^4	0.90
Titanium dioxide	300	30	5.4×10^5	0.12

US should be used carefully because it can induce damage to the carbon nanotubes (defects and even scission).

To quantify the energy input required for deagglomeration, most authors selected the specific energy, E_v, to link to the final mean diameter (Table 25.1). E_v is defined as

$$E_v = \frac{E}{V} = \frac{Pt}{V}$$

(25.2)

E_v (J/L) takes into account the energy provided E (power of US multiplied by the sonication time) and the sonicated volume V. However, it is important to note that it would be better to consider the solid content rather than the suspension volume (Le et al., 2013b).

25.4.2 Disruption and breakage

In addition to particle separation (deagglomeration and dispersion), US can also lead to particle disruption and breakage. Some analogy with mechanical effects in ultrasonic cleaning may be pointed out. Despite its widespread use, the associated physical phenomena have not been conveniently analyzed. Nevertheless, it is recognized that the main observed phenomenon under low-frequency US is erosion (Mason et al., 2011). The microjets emanating from the asymmetric collapse of the transient cavitation bubbles achieve particle surface erosion, leading to fines production. However, particle breaking can occur as a distinct mechanism. Violent interparticle collisions when the shock occurs at a particle defect may propagate a crack and lead to particle breakage.

A recent experimental and theoretical US investigation of an alumina suspension (Raman et al., 2011) provided a kinetic model of breakage based on a Kapur function approach and determined the main mechanism. Numerical modeling of grinding was developed to predict the evolution of particle size distributions using population balance. The R_i function is defined as the cumulative oversize fraction above size x_i at time t from m_i, which is the mass fraction of particles sized x_i at time t. R_i is linked to two functions, as shown in Equation (25.3): the breakage function $B_{i,j}$, which represents the

particle size distribution resulting from the breakdown of fraction of size x_j, and the selection function S_i, that is, the probability of this size x_i to be fragmented.

$$\frac{dR_i}{dt} = -S_i R_i(t) + \sum_{j=1}^{i-1} R_j(t) \left[S_{j+1} B_{ij+1} - S_j B_{ij} \right] \tag{25.3}$$

This equation is normally solved using the similar solutions presented by Kapur (Equation (25.4)), adopting simplified expressions for B and S.

$$R(x,t) = R(x,0)\exp\left[\sum_{k=1}^{p} K^{(k)}(x)\frac{t^k}{k!} \right] \tag{25.4}$$

The term set in brackets includes what is known as the Kapur functions, from which $B_{i,j}$ and S_i can be derived.

For short grinding times, a residual ratio, representing the fraction of particles not yet broken, can be defined as Equation (25.5):

$$f(x,t) = \frac{R(x,t)}{R(x,0)} = \exp\left(K^{(1)}(x)t \right) \tag{25.5}$$

By plotting $\log\left[\frac{R(x,t)}{R(x,0)} \right]$ versus time t, it is possible to obtain the first Kapur function $K^{(1)}$ and thereby S_i and $B_{i,j}$ from Equations (25.6) and (25.7)

$$S_i = -K_i^{(1)} \tag{25.6}$$

$$B_{i,j} = \frac{K_i^{(1)}}{K_j^{(1)}} \tag{25.7}$$

By plotting the curve $B_{i,j} = f\left(\frac{x_i}{x_j}\right)$, it is possible to determine the main mechanism of breakage and compare its positions on the two extreme curves (abrasion and breakage curves) (Figure 25.5). The experimental curve is expected to lie between the two
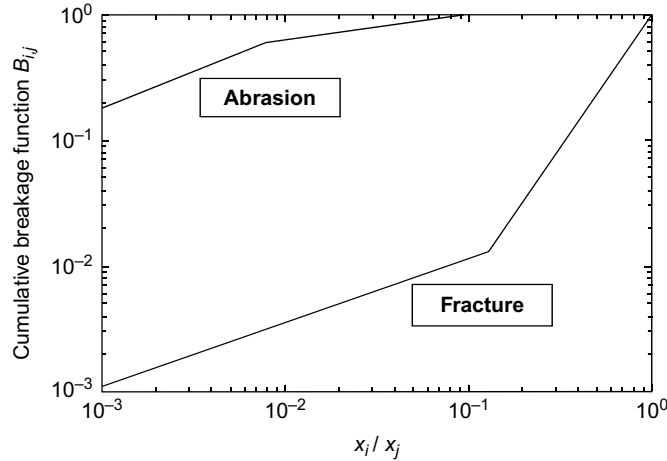

Figure 25.5 Cumulative breakage function representation $B_{i,j}$ versus x_i/x_j obtained for different grinding mechanisms according to Raman et al. (2011).

extreme curves, indicating a combination of abrasion and breakage. Under sonication the experimental curve $B_{i,j}$ is nearer to the abrasion curve, which would suggest that the dominant breakage mechanism is abrasion. However, it is important to note that it is only a qualitative analysis.

So the Kapur function takes into account the particle size. But Raman et al. (2011) proposed to include in Equation (25.8) an ultrasonic parameter a, the function of the amplitude ratio:

$$K^{(1)}(x) = -a\left(1 - \exp(-bx)\right) \tag{25.8}$$

a is connected to the amplitude ratio:

$$a = a_0 + a_1 \frac{\varepsilon}{\varepsilon_{max}} \tag{25.9}$$

where $\frac{\varepsilon}{\varepsilon_{max}}$ is the amplitude ratio (equivalent to the relative input power); a_0, a_1, and b are parameters. Referring to calorimetric measurements, the amplitude ratio variation with the specific input ultrasonic power (W/kg) was linear at a given temperature.

Monitoring patterns of population could be achieved correctly, taking into account not only particle size but also operation parameters such as temperature and US power input. It shows that even if particle abrasion is the main mechanism, fracture can occur in specific cases. Note that this model is valid only for short sonication times (10 min). Because of breakage, the number of particles increases. So, cavitation areas might be reduced because of possible damping of the acoustic intensity, even under the cavitation threshold.

US can also disrupt different types of cells. In this particular case, the objective is not to reduce the size of the element but to break the membrane in order to destroy the cell (e.g., for sterilization) or to recover products inside. Bacteria cells, for example, can be broken or lysed to recover protein. The energy liberated during bubble collapse is dissipated in eddies which, depending on their size compared to the cells, result in cell membrane deformation and erosion or in cell motion (Doulah, 1977, 1978). Kinetics of bacteria cell disruption (*Lactobacillus acidophilus*, *Acetobacter peroxydans*) based on the theory of local isotropic turbulence was proposed (Choonia and Lele, 2011; Kapucu et al., 2000). The model takes into account the sonication power. Fn, the cumulative fraction of the cells disrupted at a given acoustic power, was a function of the sonication time t:

$$\text{Fn} = 1 - \exp\left[-\left(\frac{t}{\alpha}\right)^{\beta}\right] \tag{25.10}$$

where α gives the characteristic lifetime of the equipment being tested (it is a sequential process; for example, the generator used by Kapucu et al. (2000) permits control of the wave duty cycle, which was a 4-s cycle: 2.5 s with the generator acting and 1.5 s of rest). β determines the pattern of failure: $\beta < 1$ indicates early life failure, $\beta = 1$ gives a constant failure, and $\beta > 1$ implies the failure results from wear effects. β values decreased when the acoustic power increased and so the disruption efficiency. Cell disruption was shown as directly proportional to the acoustic power. The same work

Table 25.2 Order of magnitude of required time for the disruption according to ultrasonic energy and cell nature

Particle nature	Power	Time (s)	E_v (J/L)	Lysed cells (%)
Spores	10 W/cm^2	60	—	100
Vegetative cells	0.9 W/cm^2	10	—	82
Polymer micelles	40 W	600	4.8×10^6	100

carried out on *Escherichia coli* proved US to be 22 times faster than enzymatic methods in terms of protein release (Ho et al., 2006).

Of course, the efficiency of the cell disruption process is not only dependent on the acoustic power of the sound waves but also on the physical strength of the cell wall of the microorganisms (Sauer et al., 1989). Particular attention should be paid to the control of temperature, especially close to the probe. Indeed, most of the ultrasonic energy is dissipated into the medium, and the subsequent increase in temperature can also cause the degradation of proteins. Another parameter to take into account is the size and the shape of the cell. The smaller and rounder the cell, the more difficult it is to disrupt (Alliger, 1978).

Other examples of particle disruption exist, such as polymer micelles for medical applications (Xuan et al., 2011) and spores (Chandler et al., 2001). Recent experiments show that US can induce leakage from lipid vesicles. The mechanism is not so clear: cavitation bubbles would induce transient structural deformation, resulting in the formation of transient mesopores (Marmottant et al., 2008; Wrenn et al., 2013). The few results indicating the order of magnitude of time required for the disruption according to the ultrasonic energy and the nature of the cell are reported in Table 25.2.

25.5 Solid and liquid dissolution

When no chemical reaction is involved, dissolution is usually controlled by mass transfer from the solid surface to the liquid bulk. In this case mass transfer depends on the concentration gradient (difference between equilibrium concentration at the solid surface and bulk concentration), the liquid–solid interfacial area, and the liquid–solid mass transfer coefficient. In well-mixed batch dissolution, the solid–liquid mass transfer process can be modeled by Equation (25.11):

$$\frac{dC}{dt} = k_c \left(\frac{S}{V} \right) (C^* - C) \tag{25.11}$$

where C is the concentration of solute in solution (mol/m^3), t the time (s), k_c the intrinsic mass transfer coefficient (m/s), S the surface area (m^2), V the volume of solvent (m^3), and C^* the solubility, the saturation concentration of the solute (mol/m^3).

Dissolution is usually performed by suspending the solid in the solvent under stirring, and this process may be rather slow for sparingly soluble solids. In the case of suspension, the mass transfer coefficient k_c is nearly independent of the stirring speed as long as total particle suspension has been achieved. This important feature, often ignored, may be explained by the fact that (i) k_c is connected to the relative velocity between the particles and the stirred liquid (nearly equal to the terminal velocity) and (ii) increasing turbulence by increasing stirring speed results in two opposite effects: reduced terminal velocity but increased mass transfer coefficient at a given velocity. Then very intensive stirring does not improve dissolution in suspension unless the particles break up.

High-power US may provide an efficient alternative to usual dissolution in a stirred reactor, where energy is dissipated in the whole liquid bulk. With US in cavitation conditions, because of the specific interaction between cavitation bubbles and solid particles, a much higher fraction of the energy is dissipated in the close vicinity of the particle surface. The bubble collapse near the suspended particles provides intense microstreaming and efficient renewal of the liquid in the boundary layer, leading to a much faster mass transfer coefficient. In addition, some authors have claimed that solubility C^* could also be improved under sonication, but it seems to be more likely to be an effect of the temperature increase caused by US energy input in uncontrolled temperature experiments (Sandilya and Keenan, 2012).

In Equation (25.11), the surface area S/V also will be increased if the ultrasonic break up of solid particles occurs (see Section 25.4) which can significantly enhance the whole dissolution process. Of course, the addition of these two additive effects of low-frequency power US—enhanced mass transfer coefficient and enhanced solid–liquid surface because of particle break up—will provide the best US efficiency, well above that of usual stirring.

Surprisingly, there is no specific work dedicated to liquid–solid mass transfer in suspension during sonication. Indeed, it is rather difficult to find examples of dissolution under US without resizing (breaking) the particles. Most often, erosion or break up take place simultaneously and modify the particle size distribution, generating fines particles that are rapidly dissolved. One example of non-eroded particles is the dissolution in water of crystallized salts in the pore network of stones (granite and sandstone) (Inigo et al., 2001). In this case, dissolution takes place only for one of the components present in the solid. The standard method is carried out under stirring for 3 days at a temperature of 60 °C. Using sonication, it was possible to achieve a comparable dissolution in only 45 min. However, the role of US inside the solid matrix was not explained.

Research involving the effect of US on simultaneous size reduction and dissolution of particles is scarce. Dissolution and particle size reduction of alumina and silica have been described in the context of contaminated sediment treatment (Lu et al., 2002). Sonication permits improvements in the dissolution of aluminum and silicon compared with classic mechanical stirrers (concentration after sonication is 7–20 times that of only mixing). The average particle size decreases and a new population of small particles appear. Therefore, this phenomenon cannot be explained only by dissolution. Scanning electron microscopy observations show that the solid surfaces

become smoothed as a result of sonication, confirming erosion. The two phenomena were observed but not quantified.

Interesting studies of the breakage and dissolution of sparingly soluble benzoic acid dispersed in aqueous glycerol solutions were recently performed. A smart chemical engineering approach is followed to separate break up and mass transfer effects (Sandilya and Keenan, 2012). To delineate the effects of particle breakage from solid dissolution, additional experiments without mass transfer limitation (by presaturating the solvents with benzoic acid) were carried out. Empirical correlations were developed to describe the evolution of the surface area according to the ultrasonic energy. So, it is possible to estimate the specific area and decouple the effect of sonication on the mass transfer coefficient and on surface area. A Sherwood number correlation is proposed to estimate US influence on intrinsic mass transfer coefficient k_{US}, taking into account the variation of the De Brouckere particle mean diameter (d_{43}). The Sherwood number is classically defined according to Equation (25.12):

$$Sh_{US} = \frac{k_{US}\,d_{43}}{D_{AB}}$$ (25.12)

where k_{US} is the intrinsic mass transfer coefficient under sonication, d_{43} the De Brouckere particle mean diameter (the equivalent diameter of a sphere of same volume), and D_{AB} the mass diffusivity. A Sherwood number correlation is proposed:

$$Sh_{US} = 0.6732\,(Re_{US})^{0.4360}(Sc)^{0.3366}$$ (25.13)

This correlation is based on a usual Schmidt number Sc, defined as the ratio of kinematic viscosity ν (m^2/s) and mass diffusivity D (m^2/s) and a specific US Reynolds number. Re_{US} is based on the energy dissipation ε (dissipated power per unit weight [W/kg or m^2/s^3]) and kinematic viscosity ν (m^2/s), as is often used in modeling turbulent mass transfer (Kawase and Mooyoung, 1987).

$$Re_{US} = \frac{d_{43}^{4/3}\,\varepsilon^{1/3}}{\nu}$$ (25.14)

This unique correlation could be used in any dissolution case, even when the solid is strong enough not to undergo breakage or erosion.

Another type of transfer enhancement by sonication was suggested by cellulose-improved dissolution in ionic liquids under US (Lan et al., 2011). The operating time was reduced from 190 to 20 min. In this case, US was supposed to provide a greater penetration of the ionic liquid into cellulose and increase the mass transfer. However, the conditions of dissolution might be better because of the temperature increase.

In addition to the two fundamental effects of power US on solid dissolution (mass transfer increase and particle breakage, leading to a larger solid surface), a third positive effect of US may be found in more complex situations, including reactions where the dissolution of some species may give rise to the formation of another solid that tends to coat the solid particles and then stop dissolution. In this case, US-induced

continuous erosion of the particles erodes this passivation layer and allows the dissolution process to continue.

One example in the case of zinc extraction is direct oxidative leaching of sphalerite concentrates (zinc sulfide concentrates) with ferric iron (Grenman et al., 2007). Zinc is dissolved and at the same time ferric iron is reduced to ferrous iron in a sulfuric acid solution. Using a low US frequency (30 kHz), it was assumed that no US radical chemistry was performed. Indeed, experiments carried out under strong mechanical agitation but with silent conditions gave the same results: no increase in the reaction rate. One interesting point is that under some conditions another undesired reaction can occur and form a layer of sulfur on the particle surface, hindering the dissolution reaction. However, their experimental data could be better fitted by a model that does not take into account the diffusion in this sulfur layer. This could suggest that the possible layer is continuously removed or not formed because of the sonication. Similar behaviors were observed by other researchers (Park and Fan, 2004; Trofimov et al., 2001). So it may be concluded that US-enhanced dissolution of chemicals is often the result of several beneficial effects: enhancement of the mass transfer coefficient, of the solid–liquid surface area through particle breakage, and regeneration of the active surface through intense cleaning and erosion.

The dissolution phenomenon is also concerned by the very important application of US in activated sludge treatment. Reduction and valorization of sewage sludge is a serious environmental and economic issue for which power US has become an industrial application. It is a well-studied area that has resulted in interesting reviews (Khanal et al., 2007; Le et al., 2013b; Yagci and Akpinar, 2011; Yin et al., 2004). Since 2000, full-scale application of this treatment in Germany has shown that US disintegration offers a reliable and cost-effective means for treating wastewater treatment sludge, resulting in a decrease in sludge quantity (volume and mass) and an increase in the biogas yield. It also results in a larger output of dry solids and a lower requirement for polymer/additives in the dewatering process.

The first step is floc breakage by sonication. A floc will be broken if the stress applied at its surface is larger than the bonding strength. Therefore there exists a critical ultrasonic power above which the floc structure can be disintegrated. As for a solid particle, two phenomena previously described in Section 25.4 can take place: surface erosion and large-scale fragmentation. Ultrasonic sludge treatment can be divided into two stages: first, porous flocs (100 μm) are disrupted into small microfloc aggregates or floccule with a diameter of 10–20 μm. Then, floccules are slightly reduced to a diameter <10 μm (primary particle about 2 μm), bacteria and coliform are lysed, and the intracellular organic substances are released. The two stages are not entirely separated because sludge is not homogeneous. Short periods of intense sonication are sufficient to quickly reach a stable small particle size (micron). However, if the bacteria must not be damaged, a low level of ultrasonic energy over a long time is preferred.

In addition to disintegrating cells and flocs, US also helps to dissolve organic compounds, generally quantified in terms of chemical oxygen demand (COD), during or before anaerobic digestion, which is particularly interesting for methanization. Sludge COD is the quantity of oxygen needed to fully oxidize the organic material

(mineralization) contained in the sludge (both in cells and in the various solid materials). It must be transferred from the cell content (disruption) and solid materials (solubilization) into the external liquid phase of sludge and then transformed by the anaerobic methanization process. COD and rate of nitrogen solubilization gradually increase during the sonication, as did supplied ultrasonic energy (Bougrier et al., 2005; Chang et al., 2011). However, at same specific ultrasonic energy it is better to use high power for a short time (Figure 25.6) (Le et al., 2013b). The influence of some parameters on COD dissolution has been studied by Le et al. One parameter is temperature (Le et al., 2013a). US under adiabatic conditions permits an increase in temperature, which is beneficial to the COD solubilization. The external pressure also plays an interesting role, increasing cavitation, and an optimum exists (Figure 25.7). The effect of frequency also was studied, showing an acceleration of COD dissolution at 12 kHz compared with 20 kHz. However, it was shown that the kinetics of particle size reduction was much faster and not directly correlated to COD solubilization. Reduction of mean particle size during sonication is, then, a first step to dissolve COD. More work should be performed to better understand the final US-enhanced dissolution.

Other research concerning dissolution assumes that US could increase solubility. Although remarkable results were observed, this hypothesis is very controversial and has no scientific basis: contrary to a gas–liquid system, a change of solubility in liquid–liquid or liquid–solid systems would involve some chemical change or some change in thermodynamic conditions, such as temperature. One example is whey protein. It could be solubilized more under sonication (Jambrak et al., 2008), but experiments were carried out under adiabatic conditions, so the resulting increase of temperature did contribute to enhancing the protein solubility. Moreover, sonication induced the lysis of the globular protein, which results in changes in the three-dimensional structure. This caused an increased number of charged groups
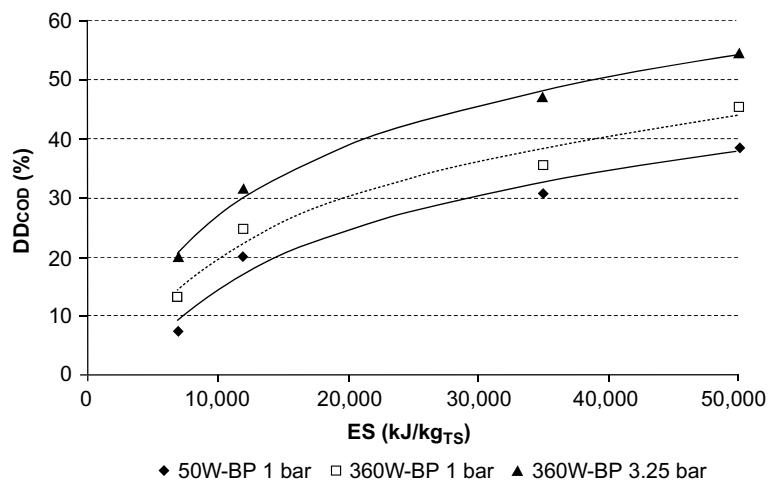

Figure 25.6 Effect of specific energy ES on COD dissolution (DD_{COD}) according to power input and external pressure according to Le et al. (2013a).
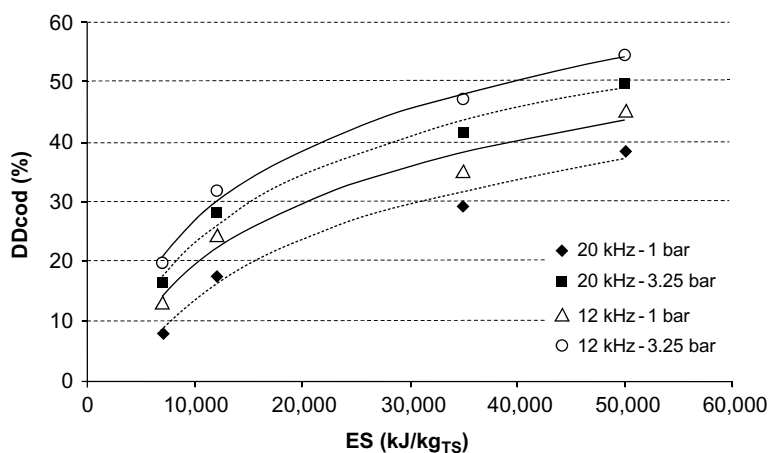
Figure 25.7 Effect of specific energy ES on COD dissolution (DD$_{COD}$) according to external pressure and frequency according to Le et al. (2013b).

(NH$_4$$^+$, COO$^-$), leading to better protein–water interaction. Again, it seems more probable that this solubility improvement under sonication is simply caused by changing the operating conditions (higher temperature) and/or modifying the nature of the product to be dissolved. In the same way, conclusions were drawn from results of dissolution of glycyrrhizic acid from glycyrrhiza uralensis in water (Yang et al., 2012). US was able to change the structure of glycyrrhiza uralensis, so a new equilibrium was reached. Another work clearly demonstrated that US does not affect the solubility of docosane in heptane (Alves et al., 2001).

To a lesser extent, examples of liquid dissolution can be found. The dissolution and reaction modeling for hydrolysis of tetraethoxysilane in a heterogeneous tetraethoxysilane–water–hydrogen chloride mixture under US stimulation was investigated (Donatti et al., 2002). US was claimed to maintain a quantity of water under a virtual state of dissolution. Sonication could induce a thermodynamic modification and create a new equilibrium. As previously explained, it is true that US generates locally a hot spot with a high temperature and pressure. So, it could change the equilibrium. But in the liquid phase, this increase in temperature is not so large (about 12°) and concerns only a small part of its volume. Under sonication, alcohol was no longer needed to promote the reaction. The explanation of the enhancement is more likely faster mixing due to cavitation. It was considered equivalent to an increase of contact area between the two phases (alkoxide and water). In the same way, US is highly recommended for producing biodiesel, and a commercial US reactor is available (Hielscher®). Achieving a fine emulsion between the two liquid phases, it improved oil–ethanol mass transfer in the reaction mixture during transesterification (Kumar et al., 2012). Sonication allows faster operation (7 min instead of the 4 h necessary for conventional techniques) under mild conditions (no high temperature and/or pressure).

25.6 Homogenization

In a chemical engineering approach, homogenization generally means "to obtain a homogeneous concentration," that is, a uniform concentration everywhere in the reactor, and most often "mixing" is preferred to homogenization. In food engineering it has a much more specific meaning: homogenization is the important process of decreasing the particle size in fluids such as milk, fruit juice, tomato products, and sauces. Classically, in the case of fat globules, the final size to reach is about 1–5 μm, whereas for solid food it is about 1–3 μm. The goal of this size reduction is to prevent the settling, agglomeration, and segregation of particles during storage to keep a good dispersion as long as possible. This provides improved product stability, shelf life, digestion, and taste. Indeed, according to the density of the dispersed phase, agglomeration leads to a higher concentration at the top (fat globules) or at the bottom (fruit pulp). Milk homogenization is essential to avoid obtaining various levels of flavor and fat concentrations. Homogenization increases viscosity and the feel of the final product in the mouth. Milk homogenization is by far the most important industrial application, and the most investigated, and this section focuses on it.

Homogenization can be performed using a high-speed blender, but a high-pressure homogenizer (100–200 bar) is conventionally used. Initial suspended particles with sizes ranging typically from 5 to 20 μm enter the homogenizer. The pressurized suspension enters through the homogenization head and is abruptly forced to change direction (angle of 90°) and pass through a smaller section. Then acceleration causes a large increase in kinetic energy, resulting in particle size reduction. The proposed mechanisms to explain this phenomenon are shear, microturbulence, and hydrodynamic cavitation. Indeed, fluid velocity dramatically increases. Because of energy conservation the pressure decreases and can become lower than liquid vapor pressure, leading to the formation of cavitation microbubbles, which later collapse in higher-pressure zones where the fluid decelerates.

Therefore it is logical to use US to benefit of the acoustic cavitation effects (Herceg et al., 2009; Mason et al., 1996; Villamiel and de Jong, 2000). The disruption of fat globules is still caused by pressure differences due to collapsing bubbles (shockwaves and microjets). This breakage is not spectacular because the mean particle size is not decreased much. In general, the average size has to be reduced from 10 to <1 μm under sonication. The objective is principally to break large particles to obtain a very narrow final size distribution and to form a homogeneous suspension. Homogenization can be controlled through the variance of the particle size distribution generally fitted by a log normal law. In addition to the particle size reduction, the location of fat is also determined after 2 days in a refrigerator: fat contents of the sample from the upper part, that one-tenth (a), and from the bottom nine-tenths (b). Therefore, the homogenization efficiency is defined as shown in Equation (25.15):

$$H_e = \frac{a-b}{a} \times 100 \tag{25.15}$$

A lower H_e indicates better homogenization. A diameter around 0.8 μm seems to be convenient for avoiding a creaming effect during storage.

The mean globule size and H_e decrease rather quickly with the sonication time (diameter around ≤ 1 μm within ≤ 15 min). This process is even faster at high US power, as shown in Table 25.3 (Ertugay and Sengul, 2004), which compares fat globule diameters obtained in conventional and ultrasonic homogenization treating an equivalent quantity of milk. Sonication for 10 min at 180 W obtains smaller-diameter fat globules than conventional homogenization at 200 bar.

US also has a very good effect on homogenization compared with conventional homogenizers, but only at high power levels (>180 W during 5 min to treat 250 mL of milk). It should be noted that for the same energy the best results are obtained at the highest power and the shortest time. Such results also were found by Le et al. for sludge disintegration (see Section 25.4).

The breakage mechanism is not clear because milk is a complex fluid. Milk fat globules are quite spherical although delimited with a membrane. US waves disrupt and crack this membrane by releasing triacylglycerols. Indeed, electronic microscope observations of raw milk fat globules show very circular particles with a smooth surface. After sonication the globules are very small (diameter of <1 μm), are no longer spherical, and have orifices visible on their surface. Moreover, this surface is completely roughened and granular. This can be caused by the interaction between the disrupted milk fat globule membrane and some casein micelles existing in the milk. These micelles coat the fat globule surface. So the suspension homogenization is more stabled during the time. Consequently, sonication also modifies milk's composition and thus its physical properties such as viscosity and pH (Michalski and Januel, 2006; Shanmugam et al., 2012).

Much research in the field of homogenization of milk of different origins (animal, vegetable, and sometimes human; skim or not) resulted in the same US efficiency even if the fat content (0.6–4%) and globule size of these milks differ slightly (Bosiljkov et al., 2009, 2011; Ertugay and Sengul, 2004; Silva et al., 2011; Wu et al., 2000). Some examples of homogenization conditions are presented in Table 25.4.

An interesting operation is thermosonication; milk can be pasteurized and homogenized in a single step, providing important cost savings (Bermudez-Aguirre et al., 2008; Czank et al., 2010). A synergy could be observed. Indeed, as described in Section 25.4, US can disrupt biological structures and cause cell death. Moreover, operation under adiabatic conditions leads to an increase in temperature due to high power dissipation. From a nutritional point of view, the combination of US and heat is a food preservation technique that retains higher quantities of bioactive components compared with common thermal pasteurization practices (Earnshaw et al., 1995; Miles et al., 1990). One proposal could be to use sonication alone to both homogenize and pasteurize. However, research seems to indicate that sonication alone is not sufficient as a nonthermal alternative to pasteurization. US was found to eliminate spoilage and reduce potential pathogens to zero or to acceptable levels, but it is ineffective in deactivating some enzymes such as alkaline phosphatase and lactoperoxidase (Cameron et al., 2009).

Table 25.3 Fat globule diameters obtained in conventional and ultrasonic homogenization

Treatment	Raw milk	Conventional homogenization	Ultrasonic homogenization Power (W) Time (min)							
			90 5	90 10	180 5	180 10	360 5	360 10	450 5	450 10
Mean fat globules size (μm)	5.5	(Alfa Laval homogenizer 200 bar) 2.63	3.88	3.5	3.38	2.38	2.13	1.25	1.13	0.72

Table 25.4 Times classically required to homogenize different type of milk

Milk origin	Time (min)	Fat globule diameter (µm)	Power input (W)	Volume (mL)
Cow	10	1.25	360	250
Soybean	10	1.5	100	150

Table 25.5 Particle diameters obtained in 200 mL tomato juice after 8 min under sonication versus the input power

Sonication power (W)	0	60	90	120
Particle size (µm)	423	371	70	58

Source: Wu et al. (2008).

Others research on homogenization of other food suspensions such as fruit juice, tomato products, and sauces also were carried out. Texture is a critical quality attribute in consumer acceptability (Cao et al., 2010; Luisina Gomez et al., 2011). The objective of ultrasonic treatment in this case is to significantly enhance the total solid content; viscosity is more the key parameter (Anese et al., 2013; Vercet et al., 2002; Wu et al., 2008). In some cases the particle size distribution is followed by chord length distribution as a function of US intensity. Pulsed US with a short on/off sequence (5 s), for a total sonication time of few minutes, was preferred (Keenan et al., 2012). As another example, tomato juice (200 mL) was sonicated for 8 min at different power inputs (Wu et al., 2008). The resulting mean diameters are presented in Table 25.5.

One last point is that the use of US has a slight limitation because of equipment. The risk of metal contamination because of probe erosion is an important drawback of these applications. Such metal contamination is totally prohibited in the food industry, which is very controlled. A possible design would be to use many transducers of rather low power dispatched around the US homogenizer diameter to focus US in the central zone, where cavitation would take place, and to avoid it at the emitter surfaces (Dion, 2009).

25.7 Emulsification

An emulsion is a heterogeneous system consisting of at least one immiscible liquid intimately dispersed in another in the form of droplets, whose diameters, in general, exceed 0.1 µm; recently, however, growing interest was focused on nanoemulsions down to 20 nm (Leong et al., 2009). Such systems are of great importance as final products in the food, pharmaceutical, and cosmetic industries and as reaction media

in emulsion polymerization or for extraction purposes. They may be stabilized by surface-active agents.

The type of simple emulsion (water-in-oil or oil-in-water, commonly abbreviated as w/o or o/w) is chosen mainly by the volume ratio of the two liquids, their order of addition, and the nature of the emulsifier. Nevertheless, using US favors the phase undergoing first cavitation (it has the lower cavitation threshold) to be the continuous phase. O/w emulsions are more easily prepared and most often investigated. Note that three-phase o/w/o emulsions also were prepared by ultrasonic vibration (Lin and Chen, 2008).

Emulsions may remain practically unchanged to the naked eye for several months but eventually return to their stable state, that is, a phase-separated system. In emulsion breaking, two kinds of phenomena can be discriminated: those that are generally reversible and involve particle aggregation and migration (by Stoke's law), and those that are irreversible and related to particle size modification (through Ostwald ripening and coalescence). Briefly, emulsion stability depends on (i) droplet size, (ii) difference in the density of the dispersed and continuous phases, (iii) viscosity of the continuous phase, and, above all, (iv) the electrostatic and/or steric repulsion between droplets (in which the surfactant plays a major role).

Except in special cases where spontaneous emulsification can occur, energy must be supplied to produce such metastable mixtures. A much larger amount of energy, with respect to the thermodynamic part ($\Delta G = \gamma \Delta A$) is required; the excess energy is dissipated as heat. Energy may be provided through various means, namely mechanical agitation (stirrer, colloid mill, mixer, valve homogenizer) and US. Emulsification is one of the oldest applications of high-power US (Wood and Loomis, 1927), and the first patent was granted in 1944 in Switzerland. US emulsification is thus an already known phenomenon, has been reviewed by Canselier et al. (2002), and is still largely investigated (Chiu et al., 1997; Cucheval and Chow, 2008; Freitas et al., 2005, 2006; Gaikwad and Pandit, 2008; Jafari et al., 2006, 2007; Leong et al., 2009; Lin and Chen, 2008; Mosavian and Hassani, 2010).

25.7.1 Specific aspects of US emulsification

Most of the main features and main parameters of emulsification are still expected in US emulsification: role of the surfactant, the energy supply, the physicochemical properties of the two phases (mainly density, viscosity, and surface tension), and the volume fraction of the dispersed phase. Recall that, as for previous operations described in this chapter, the energy cost should be estimated as $P_{US} \cdot t$ per volume or weight of emulsion, and the quality is mainly related to droplet size (mean diameter and distribution) and, finally, stability, which is reported much less often. Note that sono-emulsification without any surfactant, although used by Reddy and Fogler (1980) in a special emulsion system at a very low oil fraction, has not been confirmed in general.

US emulsification results from a two-step mechanism (Li and Fogler, 1978a,b). First, some drops form in the continuous phase because of Rayleigh–Taylor instability. Second, these drops progressively break into tiny droplets because of shock

waves involved by transient cavitation near the interface. The first step in creating a coarse emulsion (pre-emulsification) is the most critical concerning US efficiency (Canselier et al., 2002) because it is very dependent on geometry (Cucheval and Chow, 2008). Intense acoustic streaming performed by a small horn at a very high acoustic intensity and located near the interface (a few millimeters) in the phase to be dispersed conveniently achieves this first step. Alternatively, for example, in a large-scale operation, a gentle pre-emulsification with usual stirred or motionless equipment is needed (Abismail et al., 1999). Note that because of the limited macro-mixing achieved by US alone, a double emulsion may be generated simultaneously with w/o at the top of the beaker and o/w at the bottom (Gaikwad and Pandit, 2008).

Most often, surfactants have the desired property of being located at the cavitation bubble interface. As seen in Section 25.2, they are in contact with free radicals produced during transient collapse and might be chemically modified or even degraded (Alegria et al., 1989). Nevertheless, at a low frequency and short sonication time, this chemical degradation is not noticeable (Canselier et al., 2002; Leong et al., 2009).

A possible drawback of US emulsification, especially for food or pharmaceutical applications, is possible contamination by very small metal particles through probe erosion. Several improvements have been proposed to avoid this contamination. Freitas et al. (2006) designed a new US continuous emulsifier where US is first emitted to a steel tube containing pressurized water, which transmits the US energy to an inner glass tube where the pre-emulsified liquid–liquid mixture is flowing. This equipment is well suited for aseptic continuous processing, but because of US losses through the coupling of pressurized water and two tubes it probably is less efficient than the multiple emitter reactor, which focuses US around its axis and avoids cavitation on emitter surfaces (Dion, 2009).

The effect of pressure was noticed in very old works (Bondy and Sollner, 1935) and was especially detailed for a nanoemulsion preparation (Leong et al., 2009) for which an optimum pressure of four bar was obtained; no more emulsification occurred at higher pressures, where the transient cavitation threshold was probably not reached (Figure 25.8).

Very different results were found in some previous work (Behrend and Schubert, 2001), but it should be emphasized that the effect of pressure depends on many other conditions controlling cavitation. Cavitation intensity is connected with pressure in a rather complex way, leading to an optimum pressure, which is a function of liquid properties and gas content and acoustic density; such complex dependence should be expected for US emulsification. Thus this optimum pressure depends on temperature, the nature of the dissolved gases, the boiling point of the continuous phase, and probably the selected surfactant.

25.7.2 Main features of US emulsification

In addition to general physicochemical parameters (surfactant nature and concentration, viscosity and density of the two phases), the main operation parameter concerns energy consumption. According to turbulence theory, the maximum particle size in turbulent flow is proportional to $P_v^{-0.4}$ (where P_v is the power density). This
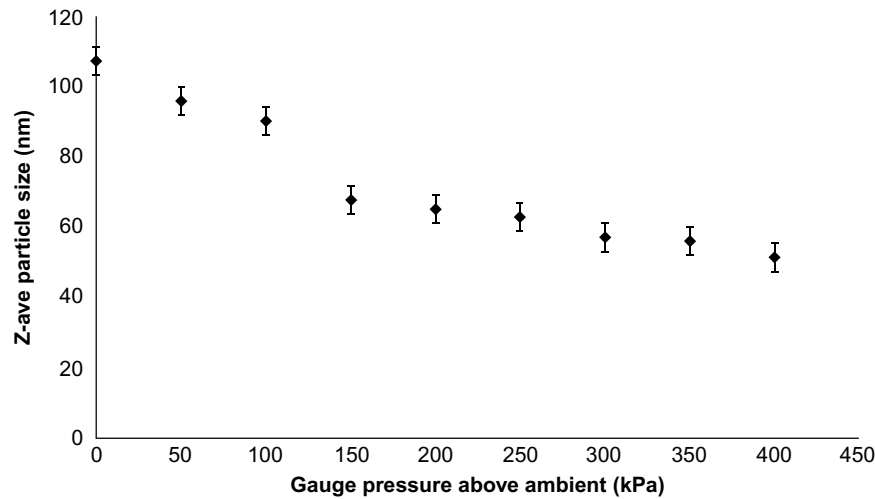
Figure 25.8 Effect of increasing overpressure in the continuous flow-through cell on emulsion particle size, according to Leong et al. (2009).

corresponds to a final stage, and in any emulsification processes the operation time (here sonication time t_e) has to be accounted for, and the energy density ($E_v = P_v \cdot t_e$ in kJ/m^3) is the key parameter to estimate the efficiency of a given emulsion formula. Most recent works use this parameter instead of separate irradiated time and US power. Nevertheless, note that previous works related to similar US applications (cell disruption, sludge disintegration) showed a slight improvement when using higher power during a shorter time at the same E_v (Le et al., 2013b). Importantly, that US emulsification does not occur at all under the transient cavitation threshold means that US is not convenient for performing coarse emulsion at low energy consumption. Above this minimum energy, most results agreed with the $P_v^{-0.4}$ dependence on mean particle diameter, whatever the US equipment, but when operating at a higher pressure a better effect of dissipated power ($P_v^{-0.6}$) was found, showing trends very similar to those of high-pressure homogenizers (micronizer) (Leong et al., 2009) (Figure 25.9).

A rather complete comparison of US and Ultra Turrax emulsification (operating according to the principle of a turbine, the dispersion head draws liquid upward then rejects the product laterally through the slots of the stator) on a simple three-component model system (water/kerosene/polyethoxylated [20 EO] sorbitan monostearate) (Abismail et al., 1999) is summarized by Figures 25.10–25.13. It affords several interesting results in favor of the US technique: (i) much smaller average drop sizes d_{32} were obtained at the same energy consumption (down to 0.3 μm) (Figure 25.10) with less polydispersion (Figure 25.11) at any dispersed volume fraction (Figure 25.12); (ii) for a given desired diameter, the surfactant amount required was reduced (about five times less; Figure 25.13); and (iii) as expected with the previous improvements, stability was greatly improved, as quantified using a Turbiscan MA 2000, an optical analyzer that is able to detect the phenomena of migration of the
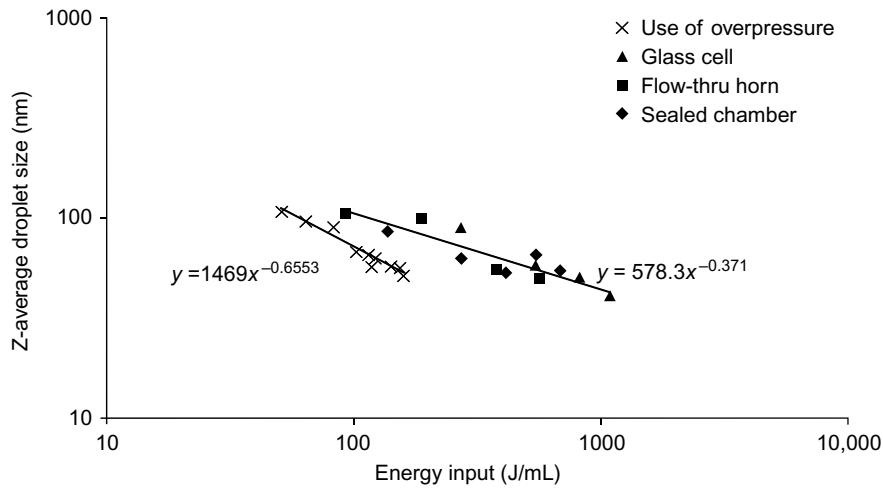
Figure 25.9 Relationship between the specific energy input and droplet size according to Leong et al. (2009).
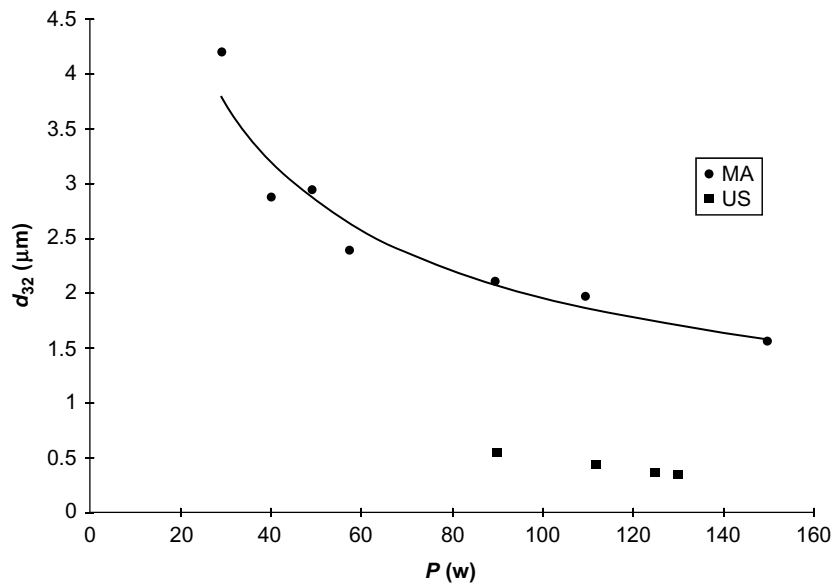

Figure 25.10 Variations of d_{32} versus power (MA, mechanical agitation; US, power ultrasound, $t = 30$ s, $c = 10$ g/L, $\varphi = 0.25$), according to Abismail et al. (1999).

particles in the medium: creaming, sedimentation, clarification, and coalescence at the beginning. The need for much less surfactant could be linked to the intense foaming that occurred when using the Ultra Turrax and captured a large amount of surfactant. Most of these findings have been confirmed by other works (Cucheval and Chow, 2008; Freitas et al., 2005; Gaikwad and Pandit, 2008; Jafari et al., 2006, 2007;
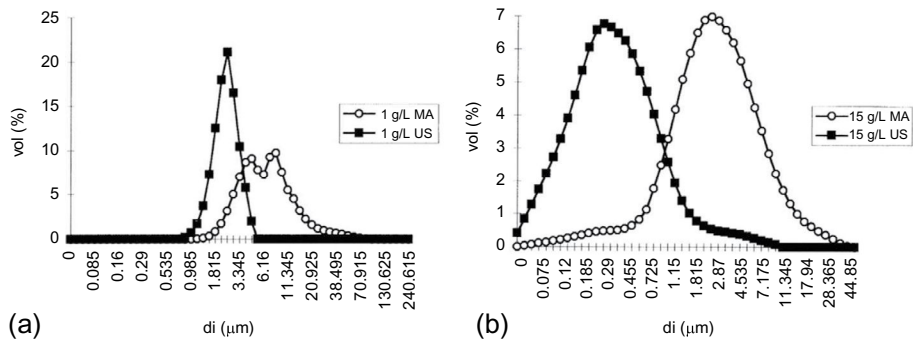
Figure 25.11 Volume drop size distribution: (a) low surfactant concentration, (b) high surfactant concentration (MA, mechanical agitation; US, power ultrasound), according to Abismail et al. (1999).

Mosavian and Hassani, 2010). Interestingly, continuous US emulsification proved to be as efficient as batch operation (Abismail et al., 2000; Freitas et al., 2006; Leong et al., 2009) with the same performance at the same energy density, as shown in Figure 25.14. This important result confirms that the main operation parameter is the energy density, which should be kept constant in any scale-up procedure, as for other emulsification techniques, while keeping in mind to largely overpass the transient cavitation threshold.
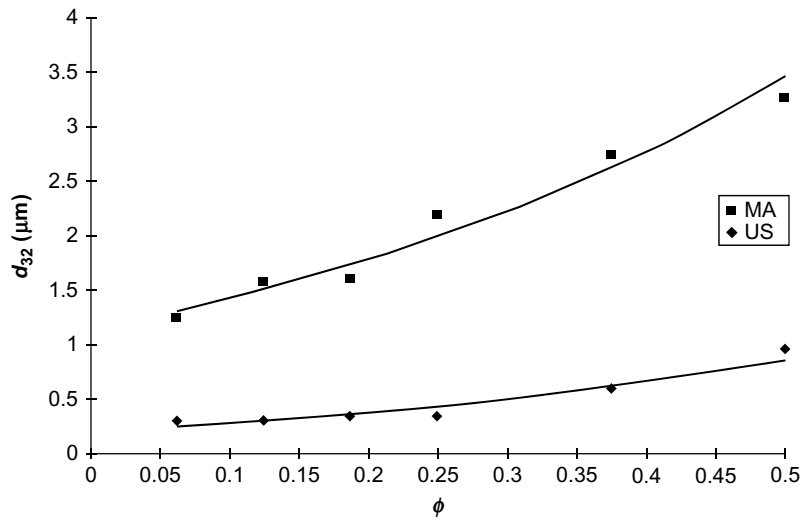

Figure 25.12 Variation of d_{32} versus oil fraction ($t = 30$ s, $c = 10$ g/L, PMA $= 170$ W, PUS $= 130$ W) (MA, mechanical agitation; US, power ultrasound), according to Abismail et al. (1999).
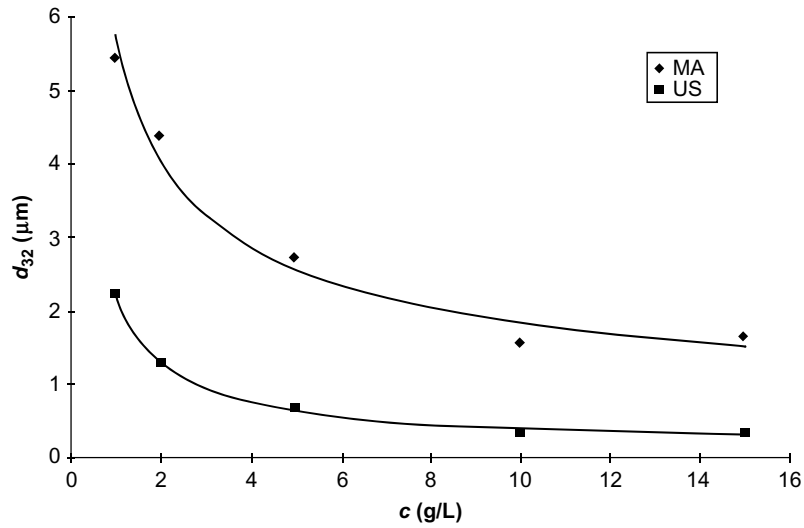
Figure 25.13 Variations of d_{32} versus surfactant concentration (MA, mechanical agitation, US, power ultrasound) ($t = 30$ s, $\varphi = 0.25$, PMA $= 170$ W, PUS $= 130$ W), according to Abismail et al. (1999).
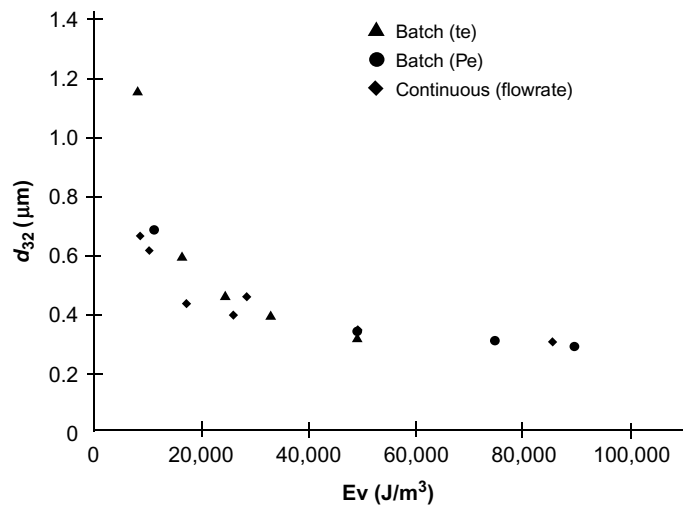

Figure 25.14 Variation of d_{32} versus energy density (varying emulsification time ($P = 130$ W), varying power ($t = 30$ s); varying flowrate ($P = 170$ W)), according to Canselier et al. (2002).

25.8 Conclusions and future trends

This chapter reviews how US can improve mixing, disruption, dissolution, homogenization, and emulsification through transient cavitation and the high concentration of energy provided by bubble collapses. Despite convenient micromixing performance, because of microeddies on the same scale as cavitation bubbles, it should be emphasized that US mixing of a single liquid phase is clearly less attractive than other applications involving a multiphase system, such as solid–liquid or liquid–liquid suspensions. Indeed, the great advantage of acoustic cavitation when compared with other means of providing energy to a multiphase system is the preferential action of collapsing bubbles near interfaces (which may be caused by easier nucleation) and their attraction toward the interface during asymmetrical collapse, achieving much better local mass and momentum transfers, which lead to faster dissolution, erosion, or breakage.

Among the future possible improvements of US applications in solid and liquid suspensions, the use of higher static pressure conditions (up to a few bar) and of ultra-low US frequency (well below 20 kHz) seem very promising, according to detailed comparisons on sludge breakup and organic dissolution (Le et al., 2013b).

From a more fundamental point of view there is still a large gap between fundamental knowledge of single-bubble cavitation and the actual complex hydrodynamics of acoustic bubble clouds in suspensions. The dynamics of a single acoustic bubble are well known, especially because of the wide interest in sono-luminescence. It may explain the high temperatures and pressures reached in the bubbles at the final point of collapse and then the chemical activity through radical formation. Nevertheless, for any US application in processing, in a cavitating medium the bubble population dynamics are extremely complex because of the bubble interactions in clouds (Tervo et al., 2006) and high acoustic damping in cavitation; the acoustic field is highly disturbed by cavitation (Dahnke et al., 1999). In addition, it is noteworthy that acoustic multibubble measurements in high cavitation conditions always show smaller diameters than expected by single-bubble dynamics at the strongest collapse conditions (Tsochatzidis et al., 2001). Using complex cavitation equipment, the main measurement of cavitation was performed with hydrophones (Harris, 1996) to record and analyze noise spectra, but the link with turbulence characteristics and resulting mass and momentum transfers has not been identified. In addition, specific features of cavitation in suspensions have not been conveniently investigated. This difficult task, which is very useful for a rational approach to any particle, drop, and cell process, should attract more sonochemical engineers.

References

Abismail, B., Canselier, J.P., Wilhelm, A.M., Delmas, H., Gourdon, C., 1999. Emulsification by ultrasound: drop size distribution and stability. Ultrason. Sonochem. 6, 75–83.

Abismail, B., Canselier, J.P., Wilhelm, A.M., Delmas, H., Gourdon, C., 2000. Emulsification processes: on-line study by multiple light scattering measurements. Ultrason. Sonochem. 7, 187–192.

Alegria, A.E., Lion, Y., Kondo, T., Riesz, P., 1989. Sonolysis of aqueous surfactant solutions—probing the interfacial region of cavitation bubbles by spin trapping. J. Phys. Chem. 93, 4908–4913.

Alliger, H., 1978. New methods in ultrasonic processing. Am. Lab. 10, 81–87.

Alves, K.C.M., Condotta, R., Giulietti, M., 2001. Solubility of docosane in heptane. J. Chem. Eng. Data 46, 1516–1519.

Anese, M., Mirolo, G., Beraldo, P., Lippe, G., 2013. Effect of ultrasound treatments of tomato pulp on microstructure and lycopene in vitro bioaccessibility. Food Chem. 136, 458–463.

Ashokkumar, M., 2011. The characterization of acoustic cavitation bubbles—an overview. Ultrason. Sonochem. 18, 864–872.

Baldyga, J., Bourne, J.R., 1984. A fluid mechanical approach to turbulent mixing and chemical reaction part ii micromixing in the light of turbulence theory. Chem. Eng. Commun. 28, 243–258.

Bang, J.H., Suslick, K.S., 2010. Applications of ultrasound to the synthesis of nanostructured materials. Adv. Mater. 22, 1039–1059.

Behrend, O., Schubert, H., 2001. Influence of hydrostatic pressure and gas content on continuous ultrasound emulsification. Ultrason. Sonochem. 8, 271–276.

Bermudez-Aguirre, D., Mawson, R., Barbosa-Canovas, G.V., 2008. Microstructure of fat globules in whole milk after thermosonication treatment. J. Food Sci. 73, E325–E332.

Bondy, C., Sollner, K., 1935. On the mechanism of emulsification by ultrasonic waves. Trans. Faraday Soc. 31, 835–843.

Bosiljkov, T., Brncic, M., Tripalo, B., Karlovic, S., Ukrainczyk, M., Jezek, D., and Brncic, S. R., 2009. Impact of ultrasound-enhanced homogenization on physical properties of soybean milk. In: Pierucci, S. (Ed.). Icheap-9: 9th International Conference on Chemical and Process Engineering, Pts 1–3.

Bosiljkov, T., Tripalo, B., Brncic, M., Jezek, D., Karlovic, S., Jagust, I., 2011. Influence of high intensity ultrasound with different probe diameter on the degree of homogenization (variance) and physical properties of cow milk. Afr. J. Biotechnol. 10, 34–41.

Bougrier, C., Carrere, H., Delgenes, J.P., 2005. Solubilisation of waste-activated sludge by ultrasonic treatment. Chem. Eng. J. 106, 163–169.

Brotchie, A., Grieser, F., Ashokkumar, M., 2010. Characterization of acoustic cavitation bubbles in different sound fields. J. Phys. Chem. B 114, 11010–11016.

Burdin, F., Tsochatzidis, N.A., Guiraud, P., Wilhelm, A.M., Delmas, H., 1999. Characterisation of the acoustic cavitation cloud by two laser techniques. Ultrason. Sonochem. 6, 43–51.

Cameron, M., Mcmaster, L.D., Britz, T.J., 2009. Impact of ultrasound on dairy spoilage microbes and milk components. Dairy Sci. Technol. 89, 83–98.

Canselier, J.R., Delmas, H., Wilhelm, A.M., Abismail, B., 2002. Ultrasound emulsification—an overview. J. Dispers. Sci. Technol. 23, 333–349.

Cao, S., Hu, Z., Pang, B., Wang, H., Xie, H., Wu, F., 2010. Effect of ultrasound treatment on fruit decay and quality maintenance in strawberry after harvest. Food Control 21, 529–532.

Chandler, D.P., Brown, J., Bruckner-Lea, C.J., Olson, L., Posakony, G.J., Stults, J.R., Valentine, N.B., Bond, L.J., 2001. Continuous spore disruption using radially focused, high-frequency ultrasound. Anal. Chem. 73, 3784–3789.

Chang, T.-C., You, S.-J., Damodar, R.A., Chen, Y.-Y., 2011. Ultrasound pre-treatment step for performance enhancement in an aerobic sludge digestion process. J. Taiwan Inst. Chem. Eng. 42, 801–808.

Chartier, T., Jorge, E., Boch, P., 1991. Ultrasonic deagglomeration of Al_2O_3 and $BaTiO_3$ for tape casting. J. Phys. III 1, 689–695.

Cheng, Q., Debnath, S., Gregan, E., Byrne, H.J., 2010. Ultrasound-assisted SWNTs dispersion: effects of sonication parameters and solvent properties. J. Phys. Chem. C 114, 8821–8827.

Chiu, Y.C., Chang, C.N., Lin, J.G., Huang, S.J., 1997. Alkaline and ultrasonic pretreatment of sludge before anaerobic digestion. Water Sci. Technol. 36, 155–162.

Choonia, H.S., Lele, S.S., 2011. Beta-galactosidase release kinetics during ultrasonic disruption of *Lactobacillus acidophilus* isolated from fermented *Eleusine coracana*. Food Bioprod. Process. 89, 288–293.

Cucheval, A., Chow, R.C.Y., 2008. A study on the emulsification of oil by power ultrasound. Ultrason. Sonochem. 15, 916–920.

Czank, C., Simmer, K., Hartmann, P.E., 2010. Simultaneous pasteurization and homogenization of human milk by combining heat and ultrasound: effect on milk quality. J. Dairy Res. 77, 183–189.

Dahnke, S., Swamy, K.M., Keil, F.J., 1999. Modeling of three-dimensional pressure fields in sonochemical reactors with an inhomogeneous density distribution of cavitation bubbles. Comparison of theoretical and experimental results. Ultrason. Sonochem. 6, 31–41.

De Castro, M.D.L., Riego-Capote, F., 2007. Ultrasound-assisted crystallization (sonocrystallization). Ultrason. Sonochem. 14, 717–724.

Dion, J.-L., 2009. Contamination-free high capacity converging waves sonoreactors for the chemical industry. Ultrason. Sonochem. 16, 212–220.

Doktycz, S.J., Suslick, K.S., 1990. Interparticle collisions driven by ultrasound. Science 247, 1067–1069.

Donatti, D.A., Ruiz, A.I., Vollet, D.R., 2002. A dissolution and reaction modeling for hydrolysis of TEOS in heterogeneous TEOS-water-HCl mixtures under ultrasound stimulation. Ultrason. Sonochem. 9, 133–138.

Doulah, M.S., 1977. Mechanism of disintegration of biological cells in ultrasonic cavitation. Biotechnol. Bioeng. 19, 649–660.

Doulah, M.S., 1978. Application of statistical-theory of reliability to yeast-cell disintegration in ultrasonic cavitation. Biotechnol. Bioeng. 20, 1287–1289.

Earnshaw, R.G., Appleyard, J., Hurst, R.M., 1995. Understanding physical inactivation processes: combined preservation opportunities using heat, ultrasound and pressure. Int. J. Food Microbiol. 28, 197–219.

Ertugay, M.F., Sengul, M., 2004. Effect of ultrasound treatment on milk homogenisation and particle size distribution of fat. Turk. J. Vet. Anim. Sci. 28, 303–308.

Fasaki, I., Siamos, K., Arin, M., Lommens, P., Van Driessche, I., Hopkins, S.C., Glowacki, B. A., Arabatzis, I., 2012. Ultrasound assisted preparation of stable water-based nanocrystalline TiO$_2$ suspensions for photocatalytic applications of inkjet-printed films. Appl. Catal. A—Gen. 411, 60–69.

Freitas, S., Rudolf, B., Merkle, H.P., Gander, B., 2005. Flow-through ultrasonic emulsification combined with static micromixing for aseptic production of microspheres by solvent extraction. Eur. J. Pharm. Biopharm. 61, 181–187.

Freitas, S., Hielscher, G., Merkle, H.P., Gander, B., 2006. Continuous contact- and contamination-free ultrasonic emulsification—a useful tool for pharmaceutical development and production. Ultrason. Sonochem. 13, 76–85.

Gaikwad, S.G., Pandit, A.B., 2008. Ultrasound emulsification: effects of ultrasonic and physicochemical properties on dispersed phase volume and droplet size. Ultrason. Sonochem. 15, 554–563.

Gedanken, A., 2004. Using sonochemistry for the fabrication of nanomaterials. Ultrason. Sonochem. 11, 47–55.

Grenman, H., Murzina, E., Ronnholm, M., Eranen, K., Mikkola, J.P., Lahtinen, M., Salmi, T., Murzin, D.Y., 2007. Enhancement of solid dissolution by ultrasound. Chem. Eng. Process. 46, 862–869.

Guo, Z., Jones, A.G., Li, N., Germana, S., 2007. High-speed observation of the effects of ultrasound on liquid mixing and agglomerated crystal breakage processes. Powder Technol. 171, 146–153.

Harris, G.R., 1996. Are current hydrophone low frequency response standards acceptable for measuring mechanical/cavitation indices? Ultrasonics 34, 649–654.

Herceg, Z., Brncic, M., Jambrak, A.R., Brncic, S.R., Badanjak, M., Sokolic, I., 2009. Possibility of application high intensity ultrasound in milk industry. Mljekarstvo 59, 65–69.

Hereter, A., Josa, R., Candela, X., 2002. Changes in particle-size distribution influenced by organic matter and mechanical or ultrasonic dispersion techniques. Commun. Soil Sci. Plant Anal. 33, 1351–1362.

Hihn, J.Y., Doche, M.L., Mandroyan, A., Hallez, L., Pollet, B.G., 2011. Respective contribution of cavitation and convective flow to local stirring in sonoreactors. Ultrason. Sonochem. 18, 881–887.

Ho, C.W., Chew, T.K., Ling, T.C., Kamaruddin, S., Tan, W.S., Tey, B.T., 2006. Efficient mechanical cell disruption of *Escherichia coli* by an ultrasonicator and recovery of intracellular hepatitis B core antigen. Process Biochem. 41, 1829–1834.

Inigo, A.C., Alonso, R., Vicente-Tavera, S., 2001. Dissolution of salts crystallised in building materials using ultrasound: an alternative to NORMAL (1983) standard methodology. Ultrason. Sonochem. 8, 127–130.

Jafari, S.M., He, Y.H., Bhandari, B., 2006. Nano-emulsion production by sonication and microfluidization—a comparison. Int. J. Food Prop. 9, 475–485.

Jafari, S.M., He, Y., Bhandari, B., 2007. Production of sub-micron emulsions by ultrasound and microfluidization techniques. J. Food Eng. 82, 478–488.

Jambrak, A.R., Mason, T.J., Lelas, V., Herceg, Z., Herceg, I.L., 2008. Effect of ultrasound treatment on solubility and foaming properties of whey protein suspensions. J. Food Eng. 86, 281–287.

Kapucu, H., Gulsoy, N., Mehmetoglu, U., 2000. Disruption and protein release kinetics by ultrasonication of *Acetobacter peroxydans* cells. Biochem. Eng. J. 5, 57–62.

Kawase, Y., Mooyoung, M., 1987. Solid turbulent fluid heat and mass-transfer—a unified model based on the energy-dissipation rate concept. Chem. Eng. J. Biochem. Eng. J. 36, 31–40.

Keenan, D.F., Tiwari, B.K., Patras, A., Gormley, R., Butler, F., Brunton, N.P., 2012. Effect of sonication on the bioactive, quality and rheological characteristics of fruit smoothies. Int. J. Food Sci. Technol. 47, 827–836.

Khanal, S.K., Grewell, D., Sung, S., Van Leeuwen, J., 2007. Ultrasound applications in wastewater sludge pretreatment: a review. Crit. Rev. Environ. Sci. Technol. 37, 277–313.

Kojima, Y., Asakura, Y., Sugiyama, G., Koda, S., 2010. The effects of acoustic flow and mechanical flow on the sonochemical efficiency in a rectangular sonochemical reactor. Ultrason. Sonochem. 17, 978–984.

Komarov, S., Oda, K., Ishiwata, Y., Dezhkunov, N., 2013. Characterization of acoustic cavitation in water and molten aluminum alloy. Ultrason. Sonochem. 20, 754–761.

Krause, B., Mende, M., Poetschke, P., Petzold, G., 2010. Dispersability and particle size distribution of CNTs in an aqueous surfactant dispersion as a function of ultrasonic treatment time. Carbon 48, 2746–2754.

Kumar, A., Gogate, P.R., Pandit, A.B., 2007. Mapping of acoustic streaming in sonochemical reactors. Ind. Eng. Chem. Res. 46, 4368–4373.

Kumar, D., Kumar, G., Johari, R., Kumar, P., 2012. Fast, easy ethanomethanolysis of *Jatropha curcus* oil for biodiesel production due to the better solubility of oil with ethanol in reaction mixture assisted by ultrasonication. Ultrason. Sonochem. 19, 816–822.

Lan, W., Liu, C.-F., Yue, F.-X., Sun, R.-C., Kennedy, J.F., 2011. Ultrasound-assisted dissolution of cellulose in ionic liquid. Carbohydr. Polym. 86, 672–677.

Le, N.T., Julcour, C., Ratsimba, B., Delmas, H., 2013a. Improving sewage sludge ultrasonic pretreatment under pressure by changing initial pH. J. Environ. Manag. 128, 548–554.

Le, N.T., Julcour-Lebigue, C., Delmas, H., 2013b. Ultrasonic sludge pretreatment under pressure. Ultrason. Sonochem. 20, 1203–1210.

Leong, T.S.H., Wooster, T.J., Kentish, S.E., Ashokkumar, M., 2009. Minimising oil droplet size using ultrasonic emulsification. Ultrason. Sonochem. 16, 721–727.

Li, M.K., Fogler, H.S., 1978a. Acoustic emulsification. 1. Instability of oil-water interface to form initial droplets. J. Fluid Mech. 88, 499–511.

Li, M.K., Fogler, H.S., 1978b. Acoustic emulsification.2. Breakup of large primary oil droplets in a water medium. J. Fluid Mech. 88, 513–528.

Lin, C.-Y., Chen, L.-W., 2008. Comparison of fuel properties and emission characteristics of two- and three-phase emulsions prepared by ultrasonically vibrating and mechanically homogenizing emulsification methods. Fuel 87, 2154–2161.

Lu, Y.F., Riyanto, N., Weavers, L.K., 2002. Sonolysis of synthetic sediment particles: particle characteristics affecting particle dissolution and size reduction. Ultrason. Sonochem. 9, 181–188.

Luisina Gomez, P., Welti-Chanes, J., Maris Alzamora, S., 2011. Hurdle technology in fruit processing. Annu. Rev. Food Sci. Technol. 2 (2), 447–465.

Marmottant, P., Biben, T., Hilgenfeldt, S., 2008. Deformation and rupture of lipid vesicles in the strong shear flow generated by ultrasound-driven microbubbles. Proc. R. Soc. A, Math. Phys. Eng. Sci. 464, 1781–1800.

Mason, T.J., Lorimer, J.P., 2002. Applied Sonochemistry: The Uses of Power Ultrasound in Chemistry and Processing. Wiley-VCH, Weinheim.

Mason, T.J., Paniwnyk, L., Lorimer, J.P., 1996. The uses of ultrasound in food technology. Ultrason. Sonochem. 3, S253–S260.

Mason, T.J., Cobley, A.J., Graves, J.E., Morgan, D., 2011. New evidence for the inverse dependence of mechanical and chemical effects on the frequency of ultrasound. Ultrason. Sonochem. 18, 226–230.

Mastikhin, I.V., Arbabi, A., Newling, B., Hamza, A., Adair, A., 2012. Magnetic resonance imaging of velocity fields, the void fraction and gas dynamics in a cavitating liquid. Exp. Fluids 52, 95–104.

Michalski, M.-C., Januel, C., 2006. Does homogenization affect the human health properties of cow's milk? Trends Food Sci. Technol. 17, 423–437.

Miles, C.A., Shore, D., Langley, K.R., 1990. Attenuation of ultrasound in milks and creams. Ultrasonics 28, 394–400.

Moholkar, V.S., Sable, S.P., Pandit, A.B., 2000. Mapping the cavitation intensity in an ultrasonic bath using the acoustic emission. AIChE J. 46, 684–694.

Monnier, H., Wilhelm, A.M., Delmas, H., 1999a. Influence of ultrasound on mixing on the molecular scale for water and viscous liquids. Ultrason. Sonochem. 6, 67–74.

Monnier, H., Wilhelm, A.M., Delmas, H., 1999b. The influence of ultrasound on micromixing in a semi-batch reactor. Chem. Eng. Sci. 54, 2953–2961.

Monnier, H., Wilhelm, A.M., Delmas, H., 2000. Effects of ultrasound on micromixing in flow cell. Chem. Eng. Sci. 55, 4009–4020.

Mosavian, M.T.H., Hassani, A., 2010. Making oil-in-water emulsions by ultrasound and stability evaluation using Taguchi method. J. Dispers. Sci. Technol. 31, 293–298.

Murugan, R.V., Nagarajan, R., 2008. Pulsed ultrasonic mixing: an experimental study. Chem. Eng. Res. Design 86, 454–460.

Park, A.H.A., Fan, L.S., 2004. CO_2 mineral sequestration: physically activated dissolution of serpentine and pH swing process. Chem. Eng. Sci. 59, 5241–5247.

Parvizian, F., Rahimi, M., Faryadi, M., 2011. Macro- and micromixing in a novel sonochemical reactor using high frequency ultrasound. Chem. Eng. Process. 50, 732–740.

Parvizian, F., Rahimi, M., Azimi, N., 2012. Macro- and micromixing studies on a high frequency continuous tubular sonoreactor. Chem. Eng. Process. 57–58, 8–15.

Pohl, M., Hogekamp, S., Hoffmann, N.Q., Schuchmann, H.P., 2004. Dispersion and deagglomeration of nanoparticles with ultrasound. Chem. Ing. Tech. 76, 392–396.

Pohl, B., Jamshidi, R., Brenner, G., Peuker, U.A., 2012a. Characterization of the mixing and precipitation of sonochemical flow reactors under special consideration of the reactor geometry. Chem. Ing. Tech. 84, 70–80.

Pohl, B., Jamshidi, R., Brenner, G., Peuker, U.A., 2012b. Experimental study of continuous ultrasonic reactors for mixing and precipitation of nanoparticles. Chem. Eng. Sci. 69, 365–372.

Prozorov, T., Prozorov, R., Suslick, K.S., 2004. High velocity interparticle collisions driven by ultrasound. J. Am. Chem. Soc. 126, 13890–13891.

Raman, V., Abbas, A., Zhu, W., 2011. Particle grinding by high-intensity ultrasound: kinetic modeling and identification of breakage mechanisms. AIChE J. 57, 2025–2035.

Reddy, S.R., Fogler, H.S., 1980. Emulsion stability of acoustically formed emulsions. J. Phys. Chem. 84, 1570–1575.

Roscoe, R., Buurman, P., Velthorst, E.J., 2000. Disruption of soil aggregates by varied amounts of ultrasonic energy in fractionation of organic matter of a clay Latosol: carbon, nitrogen and delta C-13 distribution in particle-size fractions. Eur. J. Soil Sci. 51, 445–454.

Ruecroft, G., Hipkiss, D., Ly, T., Maxted, N., Cains, P.W., 2005. Sonocrystallization: the use of ultrasound for improved industrial crystallization. Org. Process Res. Dev. 9, 923–932.

Sandilya, K.D., Keenan, A., 2012. Quantification of surface area and intrinsic mass transfer coefficient for ultrasound-assisted dissolution process of a sparingly soluble solid dispersed in aqueous solutions. Ultrason. Sonochem. 19, 509–521.

Sauer, T., Robinson, C.W., Glick, B.R., 1989. Disruption of native and recombinant *Escherichia-coli* in a high-pressure homogenizer. Biotechnol. Bioeng. 33, 1330–1342.

Sauter, C., Emin, M.A., Schuchmann, H.P., Tavman, S., 2008. Influence of hydrostatic pressure and sound amplitude on the ultrasound induced dispersion and de-agglomeration of nanoparticles. Ultrason. Sonochem. 15, 517–523.

Shanmugam, A., Chandrapala, J., Ashokkumar, M., 2012. The effect of ultrasound on the physical and functional properties of skim milk. Innov. Food Sci. Emerg. Technol. 16, 251–258.

Silva, A.C., Gonzalez-Mira, E., Garcia, M.L., Egea, M.A., Fonseca, J., Silva, R., Santos, D., Souto, E.B., Ferreira, D., 2011. Preparation, characterization and biocompatibility studies on risperidone-loaded solid lipid nanoparticles (SLN): high pressure homogenization versus ultrasound. Colloids Surf. B Biointerfaces 86, 158–165.

Son, Y., Lim, M., Khim, J., Ashokkumar, M., 2012. Acoustic emission spectra and sonochemical activity in a 36 kHz sonoreactor. Ultrason. Sonochem. 19, 16–21.

Suslick, K.S., Price, G.J., 1999. Applications of ultrasound to materials chemistry. Annu. Rev. Mater. Sci. 29, 295–326.

Suslick, K.S., Hyeon, T.W., Fang, M.M., 1996. Nanostructured materials generated by high-intensity ultrasound: sonochemical synthesis and catalytic studies. Chem. Mater. 8, 2172–2179.

Tervo, J.T., Mettin, R., Lauterborn, W., 2006. Bubble cluster dynamics in acoustic cavitation. Acta Acust. Acust. 92, 178–180.

Trofimov, T.I., Samsonov, M.D., Lee, S.C., Smart, N.G., Wai, C.M., 2001. Ultrasound enhancement of dissolution kinetics of uranium oxides in supercritical carbon dioxide. J. Chem. Technol. Biotechnol. 76, 1223–1226.

Tsochatzidis, N.A., Guiraud, P., Wilhelm, A.M., Delmas, H., 2001. Determination of velocity, size and concentration of ultrasonic cavitation bubbles by the phase-Doppler technique. Chem. Eng. Sci. 56, 1831–1840.

Vercet, A., Sanchez, C., Burgos, J., Montanes, L., Buesa, P.L., 2002. The effects of manothermosonication on tomato pectic enzymes and tomato paste rheological properties. J. Food Eng. 53, 273–278.

Vichare, N.P., Gogate, P.R., Dindore, V.Y., Pandit, A.B., 2001. Mixing time analysis of a sonochemical reactor. Ultrason. Sonochem. 8, 23–33.

Villamiel, M., De Jong, P., 2000. Influence of high-intensity ultrasound and heat treatment in continuous flow on fat, proteins, and native enzymes of milk. J. Agric. Food Chem. 48, 472–478.

Wood, R.W., Loomis, A.L., 1927. XXXVIII. The physical and biological effects of high-frequency sound-waves of great intensity. Philos. Mag. Ser. 7 (4), 417–436.

Wrenn, S.P., Small, E., Dan, N., 2013. Bubble nucleation in lipid bilayers: a mechanism for low frequency ultrasound disruption. Biochim. Biophys. Acta 1828, 1192–1197.

Wu, H., Hulbert, G.J., Mount, J.R., 2000. Effects of ultrasound on milk homogenization and fermentation with yogurt starter. Innov. Food Sci. Emerg. Technol. 1, 211–218.

Wu, J., Gamage, T.V., Vilkhu, K.S., Simons, L.K., Mawson, R., 2008. Effect of thermosonication on quality improvement of tomato juice. Innov. Food Sci. Emerg. Technol. 9, 186–195.

Xu, H., Zeiger, B.W., Suslick, K.S., 2013. Sonochemical synthesis of nanomaterials. Chem. Soc. Rev. 42, 2555–2567.

Xuan, J., Pelletier, M., Xia, H., Zhao, Y., 2011. Ultrasound-induced disruption of amphiphilic block copolymer micelles. Macromol. Chem. Phys. 212, 498–506.

Yagci, N., Akpinar, I., 2011. The investigation and assessment of characteristics of waste activated sludge after ultrasound pretreatment. Environ. Technol. 32, 221–230.

Yang, X., Dong, H., Yue, G., Lv, Y., Tang, J., Liu, W., 2012. Ultrasound changes solid-liquid leaching equilibrium of glycyrrhizic acid from glycyrrhiza uralensis in water. Future Mater. Res. Indus. Appl. 455–456, 721–725, Pts 1 and 2.

Yin, X., Han, P.F., Lu, X.P., Wang, Y.R., 2004. A review on the dewaterability of bio-sludge and ultrasound pretreatment. Ultrason. Sonochem. 11, 337–348.

Yusaf, T.F., Buttsworth, D.R., 2007. Characterisation of mixing rate due to high power ultrasound. Ultrason. Sonochem. 14, 266–274.